

Negative plasmon dispersion in the transition-metal dichalcogenide $2H\text{-TaSe}_2$

R. Schuster,¹ R. Kraus,¹ M. Knupfer,¹ H. Berger,² and B. Büchner¹

¹*Institute for Solid State Research, IFW Dresden, P.O. Box 270116, D-01171 Dresden, Germany*

²*Institut de Physique de la Matière Complexe, EPFL, CH-1015 Lausanne, Switzerland*

(Received 20 November 2008; published 30 January 2009)

We report about an electron energy-loss study on the dispersion of the charge-carrier plasmon in the charge-density-wave system $2H\text{-TaSe}_2$ above and below the metal-insulator transition. In both cases we find a negative slope, which is in remarkable contrast to the traditional prediction for metals based on the random-phase approximation. Possible scenarios for this intriguing phenomenon are discussed.

DOI: [10.1103/PhysRevB.79.045134](https://doi.org/10.1103/PhysRevB.79.045134)

PACS number(s): 71.45.Gm, 71.45.Lr, 78.20.-e, 78.70.-g

I. INTRODUCTION

The transition-metal dichalcogenides (TMDs) [TD_2 ($T = \text{Ta, Nb, Mo}$; $D = \text{S, Se}$)] have attracted a lot of interest for decades. This is mostly motivated by the appearance of several electronic phase transitions, most prominently (in)commensurate charge-density-wave (CDW) instabilities, or Peierls transitions,¹ and superconductivity. Despite a considerable amount of experimental and theoretical work, there is a continuing debate in particular about the origin of the CDW instability. The proposed scenarios range from nesting²—the connection of parallel sections of the Fermi surface by the CDW vector—to instabilities caused by Van Hove singularities in the density of states³ and momentum-dependent electron-phonon coupling.⁴

In addition, the interest in the TMDs is further fueled by the fact that fluctuations in the CDW order^{5,6} produce a pseudogap—a partial suppression of spectral weight in the vicinity of the Fermi level—which forms an important obstacle in the understanding of copper-based high-temperature superconductors.⁷ Not surprisingly, there are many attempts to disentangle the possible interplay and relationship between CDW order, pseudogap, and superconductivity in the TMD systems and the cuprates as well.^{8–11}

Another aspect which is characteristic of every electron gas, especially in the case of low dimensionality such as in the TMDs, refers to its collective modes—also known as plasmons. Their dispersion relation was rarely investigated so far despite its importance in the characterization of the electronic system as a whole.

The traditional method of determining the plasmon dispersion experimentally is inelastic electron scattering or electron energy-loss spectroscopy (EELS),¹² where the measured cross section, being proportional to the loss function (LF) $\Im(-1/\varepsilon(\mathbf{q}, \omega))$,¹³ provides access to the electronic properties via the dielectric function $\varepsilon(\mathbf{q}, \omega)$. Although there exist comprehensive EELS studies on the TMD systems,^{14,15} we are not aware of any report about the plasmon dispersion in a quasi-two-dimensional (2D) system that is really known to exhibit a CDW-ordered state.

In the present report we employ high-resolution EELS in transmission to investigate the plasmon dispersion in $2H\text{-TaSe}_2$ above and below its transitions to an incommensurate CDW state at $T = 122$ K and a commensurate one at $T = 90$ K.¹⁶ For all temperatures we find a redshift of the

plasmon upon increasing momentum transfer, in marked disagreement with the traditional prediction for simple metals.

II. EXPERIMENTS AND RESULTS

Single crystals were grown from Ta metal of 99.95% purity and Se of 99.999% purity by iodine vapor transport in a gradient of 660–620 °C, the crystals growing in the cooler end of the sealed quartz tubes. A very slight excess of Se was included (typically 0.2% of the charge) to ensure stoichiometry in the resulting crystals. Each experimental run lasted for 250–350 h. This procedure yielded single crystals with maximum size of $10 \times 10 \times 0.2$ mm³.

To prepare films which are thin enough for EELS in transmission, a single crystal was glued between two pieces of adhesive tape which were stripped off from each other until a film of appropriate thickness (~ 100 nm) was produced. After dissolving the glue in acetone, the sample was mounted on a standard electron microscopy grid which was then transferred to the spectrometer equipped with a flow cryostat. The measurements were carried out using a dedicated transmission electron energy-loss spectrometer¹⁷ employing a primary electron energy of 172 keV and energy and momentum resolutions of $\Delta E = 80$ meV and $\Delta q = 0.035$ Å⁻¹, respectively. The experimental setup allows also the detection of elastically scattered electrons, proving that the prepared films are indeed single crystals and proving the presence of the CDW for low temperatures via the verification of the related superstructure (see the inset of Fig. 1).

As the measured EELS intensity is isotropic within the hexagonal plane of the $2H\text{-TaSe}_2$ lattice, in agreement with the predicted D_{6h} symmetry,¹⁸ we focus only on the $\Gamma\text{-}M$ direction in the following. The LF for a broad energy range is shown in Fig. 1. In agreement with the earlier EELS studies,^{14,15} it is dominated by a broad structure around 21 eV which is attributed to the collective excitation of all valence electrons in the system. In addition we observe several interband transitions and prominent contributions from multiple plasmon losses, especially in the energy range of 40–50 eV. Finally the structure around 1 eV (indicated by the arrow in Fig. 1) is caused by the charge-carrier plasmon. Its temperature dependence was studied in detail before by optical means^{19,20} and we will elaborate its momentum dependence for temperatures above and below the crossover to the ordered state.

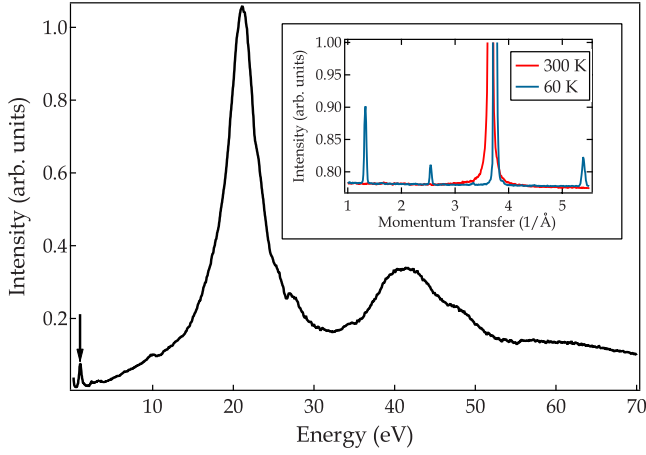


FIG. 1. (Color online) The EELS signal measured along the Γ - M direction with momentum transfer $q=0.1 \text{ \AA}^{-1}$. The arrow indicates the position of the charge-carrier plasmon. The inset shows the intensity of elastically scattered electrons where the CDW state is clearly visible by the appearance of the superstructure. The shift of the main Bragg peak around 3.6 \AA^{-1} reflects the lattice contraction upon cooling.

Being a scattering experiment, EELS always yields data which are influenced by the quasielastic line on the low-energy side of the spectrum which needs to be taken into account in order to obtain a more quantitative understanding of the low-energy region. This was done in the present work by fitting the plain spectra to a function of the form

$$I(\omega) = I_0 \{ \zeta \exp(-\eta\omega^2) + \mathcal{J}[-1/\varepsilon(\omega)] \},$$

$$\varepsilon(\omega) = 1 - \frac{\omega_p^2}{\omega^2 + i\gamma\omega}, \quad (1)$$

where ζ , η account for the steepness and width of the quasielastic line's tail and the relation for the dielectric function $\varepsilon(\omega)$ describes the Drude response of an ordinary metal, with the plasma frequency ω_p and the damping constant γ . This form of the dielectric function is motivated by the transport data on $2H$ -TaSe₂ which clearly show metallic behavior for temperatures well above its transition to the CDW state.^{21,22} Below the transition the gaps which open in the single-particle spectrum are only on the order of 20–50 meV,¹¹ which is too small to be resolved in the tail of the quasielastic line. In addition, we do not observe a pronounced redistribution of the spectral weight upon entering the CDW state. Therefore we take Eq. (1) also to fit the data measured below the transition.

The room-temperature spectra with and without the contribution of the quasielastic line are shown in Fig. 2 for momentum transfers up to $q=0.5 \text{ \AA}^{-1}$. For higher values of q the removal of the elastic line is more ambiguous and the applicability of Eq. (1) is no longer justified. Moreover there is a strongly reduced cross section which results in decreasing signal-to-noise ratios. We therefore restrict our discussion to the indicated momentum range which already captures the main results.

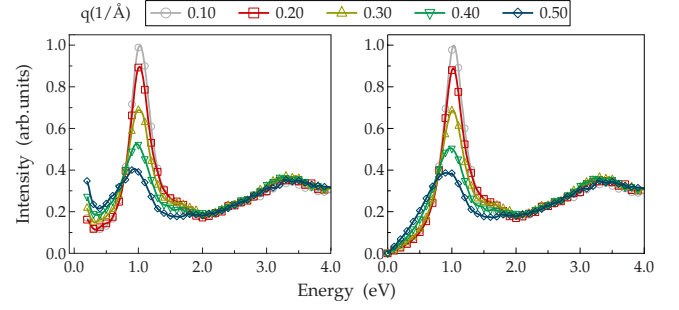


FIG. 2. (Color online) The momentum dependence of the EELS intensity along the Γ - M direction at room temperature (the spectral shapes for the CDW phase are almost unchanged) for the indicated momentum transfers. The left (right) panel shows the data before (after) the subtraction of the low-energy tail according to Eq. (1) and the spectra are normalized at the high-energy side between 4 and 5 eV.

Besides a marked reduction in spectral weight and an increasing broadening, the most remarkable observation from Fig. 2 is a small but finite redshift of the plasmon position upon increasing momentum transfer. This is a robust feature which does not depend on the normalization or the particular form of Eq. (1) as can be seen by comparing the two panels of Fig. 2. For a more quantitative understanding we extracted the peak maximum of the spectra without the elastic line as a function of momentum and the resulting plasmon dispersion is shown in Fig. 3 now for temperatures above and below the CDW transition. There is a clear downshift in the plasmon energy for all temperatures and the total bandwidth in the considered momentum range amounts to $\sim 100 \text{ meV}$ at room temperature and $\sim 150 \text{ meV}$ in the CDW phase. We found this to be a reproducible behavior and the error bars are taken as the 1σ deviation at room temperature. As the plasmon tends to sharpen at low temperatures the error bars can be considered as upper boundaries for the CDW dispersion. In addition, the onset of the dispersion is shifted to higher energies when entering the ordered state, which agrees with optical data¹⁹ that show an enhancement of the plasmon energy upon crossing the transition temperature. Campagnoli *et al.*¹⁹ could even demonstrate that this modi-

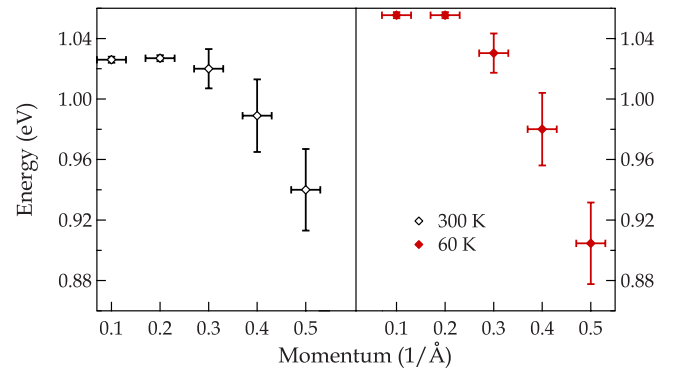


FIG. 3. (Color online) The dispersion of the charge-carrier plasmon as extracted from the local maximum of the EELS intensity measured above (left panel) and below (right panel) the transition to the CDW-ordered phase.

fication in the plasmon frequency is not caused by the lattice contraction but is rather driven by the folded single-particle spectrum in the CDW phase. However, in the remainder we focus on the negative plasmon dispersion, which is in stark contrast to the generic behavior of metals where the plasmons depend quadratically on momentum transfer, and we discuss possible reasons for this effect.

III. DISCUSSION

The conventional approach to treating the collective properties of the electron gas is the random-phase approximation (RPA) (see, e.g., Ref. 23 for an extensive treatise), where the susceptibility, which describes the response of the system to an external perturbation, is given by the Lindhard function

$$\chi^0(\mathbf{q}, \omega) = \frac{1}{V} \sum_{\mathbf{k}} \frac{n_{\mathbf{k}+\mathbf{q}}^0 - n_{\mathbf{k}}^0}{\omega_{\mathbf{k}+\mathbf{q}}^0 - \omega_{\mathbf{k}}^0 - \omega - i\delta}. \quad (2)$$

Here the $n_{\mathbf{k}}$ ($\omega_{\mathbf{k}}$) are the occupation numbers (single-particle energies) for the noninteracting system, indicated by the superscript. The dielectric function is derived from this expression via

$$\epsilon(\mathbf{q}, \omega) = 1 - v_q \chi^0(\mathbf{q}, \omega), \quad (3)$$

with $v_q = 4\pi e^2 / q^2$, the Fourier-transformed Coulomb potential. Recalling that the dielectric function describes the screening of an external potential $v_{\text{ext}}(\mathbf{q}, \omega)$ according to $v(\mathbf{q}, \omega) = \epsilon^{-1}(\mathbf{q}, \omega) v_{\text{ext}}(\mathbf{q}, \omega)$, it is clear that its zeros play an important role because they describe the collective excitations, i.e., plasmons in the system. Expanding Eq. (2) finally yields the generic behavior for the plasmon dispersion,

$$\omega_p(q) = \omega_p + \frac{\hbar}{m} \alpha q^2 + \mathcal{O}(q^4), \quad (4)$$

where α is proportional to the squared Fermi velocity.²⁴ This relation is exact in the high-density limit $r_s = (3/4\pi n)^{1/3} / a_0 \ll 1$, with the electron density n and the Bohr radius a_0 , and it is in good agreement with the experimental data for simple metals, such as Na, Li, and K.²⁵ Nevertheless it was realized that there are limitations of the RPA applicability in the range of metallic densities $r_s = 2-6$ caused by the neglect of exchange and correlation effects in the RPA, which modify the screening by the occurrence of the exchange and correlation hole: the Pauli principle and the electron-electron interaction yield a reduced density distribution around each electron. In the RPA this leads to unphysical negative values for the pair distribution function $g(r)$.²⁶ Consequently there are numerous reports about modifications of the RPA by introducing a static²⁶⁻²⁸ or dynamic²⁹⁻³³ so-called local-field correction term $G(\mathbf{q}, \omega)$ to Eq. (3):

$$\epsilon(\mathbf{q}, \omega) = 1 - \frac{v_q \chi^0(\mathbf{q}, \omega)}{1 + G(\mathbf{q}, \omega) v_q \chi^0(\mathbf{q}, \omega)}, \quad (5)$$

which effectively reduces the coefficient α in Eq. (4) and at least partially accounts for the RPA shortcomings. Numerical investigations on classical plasmas could even show a negative slope for the plasmon dispersion if the mean Coulomb

interaction between the particles exceeds a critical value.^{34,35} However, the existence of a well-defined Fermi surface¹¹ and the linear temperature dependence of the in-plane resistivity^{21,22} at room temperature strongly indicate that correlations are only of minor importance for the understanding of the electronic properties in $2H\text{-TaSe}_2$.

Another effect which may alter the plasmon dispersion is the influence of the single-particle spectrum. Experiments on the heavy alkali metals Rb and Cs showed remarkable deviations from the (until then) expected generic q^2 dependence of the plasmon energy.^{36,37} In Rb the plasmon energy stays almost constant and in Cs there is even a negative slope for small momenta, similar to our observation in Fig. 3. After considerable arguments about the importance of correlations in the alkali metals, the issue was finally settled to be a band-structure effect³⁸—with increasing atomic number the unoccupied d bands move closer to the Fermi level, which opens up the possibility of interband transitions at energies slightly above the charge-carrier plasmon. There the real part of the dielectric function can be approximated to be

$$\epsilon_1(\omega) \approx \beta(\omega - \omega_p), \quad \beta = \left(\frac{d\epsilon_1}{d\omega} \right)_{\omega_p} > 0. \quad (6)$$

Allowing for additional contributions to the screening by transitions at energies above the plasmon resonance enhances the dielectric function: $\epsilon_1(\omega) \rightarrow \epsilon_1(\omega) + \delta\epsilon_1(\omega)$. This shifts the zero of $\epsilon_1(\omega)$ —which corresponds to the plasmon energy—to lower energies proportional to $\delta\epsilon_1 / \beta$. Upon increasing momentum transfer those optically forbidden s - d transitions are enhanced by the momentum-dependent EELS matrix element,¹² thereby acquiring more and more spectral weight. This results in an effective redshift of the plasmon energy for nonzero momentum transfer.

In principle a similar effect could be at work also in $2H\text{-TaSe}_2$ considering the orbital-resolved density of states which reveals predominant Ta d and Se p states at and above the Fermi level.^{39,40} In the optical limit ($q \rightarrow 0$) the phase space for the optical absorption is therefore almost entirely formed by transitions from the chalcogen to the transition metal. This is in agreement with the reported optical data⁴¹ where the manifold of those p - d transitions shows up as two features around 3 and 5 eV. The momentum dependence of the EELS signal then would enhance the excitation probability for d - d transitions for higher q values. But this is not observed as can be seen from the fact that the EELS intensity does not change for energies above the plasmon for all measured momenta (cf. Fig. 2). Furthermore there is a report about a related compound— $2H\text{-NbS}_2$ —with a similar density of states^{42,43} that does *not* show a negative plasmon dispersion. Instead there the plasmon shows a rather strict q^2 dependence.⁴⁴ So what distinguishes these two compounds? So far it was not possible to detect any sign of CDW order in $2H\text{-NbS}_2$,²¹ and one is therefore led to speculate how the presence of the CDW may interfere with the plasmon modes.

There is a sum rule for the LF (Ref. 12) which reads

$$\int_0^\infty d\omega \omega \Im \left(-\frac{1}{\epsilon(\mathbf{q}, \omega)} \right) = \frac{\pi}{2} \omega_p^2 = \frac{2\pi^2 e^2 n}{m}. \quad (7)$$

If the integration is restricted to a finite energy range, one can gain access to the number of charge carriers contributing

to a particular transition. This value should then be *momentum independent*. If the employed normalization procedure (see caption of Fig. 2) is correct, then the integration in the energy range of the plasmon (upper cutoff energy of 1.5 eV) yields a reduction in the spectral weight of $\sim 40\%$ in the considered momentum interval, which means that a significant amount of electrons does not contribute to the plasmon excitation for $q > 0$. A possible scenario might be that there exists a maximal extension, i.e., a minimal wave vector $q_{\min} \approx 0.2\text{--}0.3 \text{ \AA}^{-1}$ of CDW-ordered areas in the $2H\text{-TaSe}_2$ lattice, which means that some electrons contribute to the formation of the CDW for $q > q_{\min}$ and therefore reduce the electron density available for the plasmon. This would also explain why the broadening of the plasmon peak sets in rather abruptly for $q \gtrsim q_{\min}$ (see Fig. 2) as the critical wave vector would also form a boundary for the onset of effective CDW-plasmon scattering. We note that precursor effects of the CDW order are visible already at temperatures far above the transition^{11,22} and the increased plasmon bandwidth in the ordered state seen in Fig. 3 would then be simply the consequence of the well-established order. However, the observation that neither the shape of the LF nor the momentum dependence of the broadening is significantly altered upon entering the CDW state cannot be reconciled within this simple picture.

Nevertheless there might be another possibility for the CDW to interfere with the plasmon dispersion. If the CDW order is present, there will be a superlattice associated with the periodicity of charge modulation. This effect may lead to a backfolding of the plasmon bands to the reduced Brillouin zone, thereby naturally producing a branch with a negative slope. Such an effect was shown to be realized in strictly 2D quantum wells⁴⁵ where a clear splitting between the different plasmon bands could be resolved in the vicinity of the zone center. For the 2D case it is well known that without any additional modulations the RPA yields an acoustic plasmon dispersion⁴⁶ with $\omega_p^{2D} \propto \sqrt{q}$ with a slope that is reduced in the presence of correlations⁴⁷ but positive for any reasonable value of the electron density. This immediately poses the questions of whether the plasmon we observe in Fig. 2 is only one branch of a more complicated band structure that should, at least, contain also an upward dispersing mode and if so, how to detect the low-energy part. We mention in addition that $2H\text{-TaSe}_2$ is only a quasi-2D system with⁴⁸ $\rho_{\perp}/\rho_{\parallel} \sim 10\text{--}50$ with ρ_{\perp} (ρ_{\parallel}) being the resistivity perpendicular (parallel) to the planes at room temperature. In contrast to other quasi-2D systems such as, e.g., $\text{Bi}_2\text{Sr}_2\text{CaCu}_2\text{O}_8$ with a much more pronounced low dimensionality of⁴⁹ $\rho_{\perp}/\rho_{\parallel} \sim \mathcal{O}(10^3)$ shows no sign of plasmon-band folding or negative dispersion. Instead there a strictly quadratic dispersion, remi-

niscient of an ordinary three-dimensional (3D) metal, is observed⁵⁰ although the tendency toward formation of the CDW instability is strongly enhanced for lower dimensionality.⁵¹

Even in one-dimensional (1D) systems where the logarithmic singularity in the susceptibility which drives the CDW instability is perfectly established, the situation is ambiguous. On the one hand the organic charge-transfer salt TTF-TCNQ (tetrathiafulvalene-tetracyanoquinodimethane), which is a typical system with a Peierls instability in the phase diagram,⁵² also shows a negative plasmon dispersion for momentum transfer along the chain axis.⁵³ Moreover in this case theory even predicted the presence of an additional (acoustic) branch⁵⁴ in the plasmon spectrum which was, however, not detected so far. On the other hand another well-known 1D system—the blue bronze $\text{K}_{0.3}\text{MoO}_3$, which is also known to undergo a Peierls transition⁵⁵—exhibits a positive slope of the plasmon dispersion for small momenta.⁵⁶

At present it is not clear what are the mechanisms that govern the CDW-plasmon interaction on a microscopic scale. We also cannot judge on a possible role of the CDW-related collective modes⁵¹ for the plasmon dynamics. In any case the fact that the presence of CDW order in $2H\text{-TaSe}_2$ is accompanied by a negative plasmon dispersion together with the observation that $2H\text{-NbS}_2$ —which is very similar to $2H\text{-TaSe}_2$ in all respects except for the CDW order—exhibits a generic metallic behavior is striking and calls for further investigations.

IV. SUMMARY

We have measured the dispersion of the charge-carrier plasmon in the CDW system $2H\text{-TaSe}_2$ for temperatures above and below the transition to the ordered state. For both cases we find a negative slope which contradicts the generic metallic behavior and is also in stark contrast to the related compound $2H\text{-NbS}_2$ which shows no CDW order. At present we cannot rule out a prominent role of the CDW order on the plasmon—though we have no microscopic understanding—as other factors which are known to influence its dynamics (single-particle spectrum and correlation effects) seem to be negligible in the present case.

ACKNOWLEDGMENTS

The technical support by R. Hübel, R. Schönfelder, and S. Leger is highly appreciated. In addition we benefited from fruitful discussions with J. Fink. This work was supported by the Swiss National Foundation for the Scientific Research within the NCCR MaNEP pool.

¹R. E. Peierls, *Quantum Theory of Solids* (Oxford University Press, New York, 1956).

²H. W. Myron and A. J. Freeman, *Phys. Rev. B* **11**, 2735 (1975).

³T. M. Rice and G. K. Scott, *Phys. Rev. Lett.* **35**, 120 (1975).

⁴M. D. Johannes and I. I. Mazin, *Phys. Rev. B* **77**, 165135 (2008).

⁵M. J. Rice and S. Strässler, *Solid State Commun.* **13**, 1389 (1973).

- ⁶P. A. Lee, T. M. Rice, and P. W. Anderson, *Phys. Rev. Lett.* **31**, 462 (1973).
- ⁷T. Timusk and B. Statt, *Rep. Prog. Phys.* **62**, 61 (1999).
- ⁸A. M. Gabovich, A. I. Voitenko, and M. Ausloos, *Phys. Rep.* **367**, 583 (2002).
- ⁹T. Kiss, T. Yokoya, A. Chainani, S. Shin, T. Hanaguri, M. Nohara, and H. Takagi, *Nat. Phys.* **3**, 720 (2007).
- ¹⁰R. A. Klemm, *Physica C* **341-348**, 839 (2000).
- ¹¹S. V. Borisenko *et al.*, *Phys. Rev. Lett.* **100**, 196402 (2008).
- ¹²S. E. Schnatterly, in *Solid State Physics* (Academic, New York, 1979), Vol. 34, pp. 275–358.
- ¹³P. M. Platzman and P. A. Wolff, in *Solid State Physics* (Academic, New York, 1973), Suppl. 13.
- ¹⁴W. Y. Liang and S. L. Cundy, *Philos. Mag.* **19**, 1031 (1969).
- ¹⁵M. G. Bell and W. Y. Liang, *Adv. Phys.* **25**, 53 (1976).
- ¹⁶D. E. Moncton, J. D. Axe, and F. J. DiSalvo, *Phys. Rev. Lett.* **34**, 734 (1975).
- ¹⁷J. Fink, *Adv. Electron. Electron Phys.* **75**, 121 (1989).
- ¹⁸D. E. Moncton, J. D. Axe, and F. J. DiSalvo, *Phys. Rev. B* **16**, 801 (1977).
- ¹⁹G. Campagnoli, A. Gustinetti, A. Stella, and E. Tosatti, *Phys. Rev. B* **20**, 2217 (1979).
- ²⁰G. Campagnoli, A. Gustinetti, A. Stella, and E. Tosatti, *Physica B & C* **99**, 271 (1980).
- ²¹M. Naito and S. Tanaka, *J. Phys. Soc. Jpn.* **51**, 219 (1982).
- ²²V. Vescoli, L. Degiorgi, H. Berger, and L. Forró, *Phys. Rev. Lett.* **81**, 453 (1998).
- ²³G. D. Mahan, *Many-Particle Physics* (Plenum, New York, 1990).
- ²⁴D. Pines, *Elementary Physics in Solids* (Benjamin, New York, 1963).
- ²⁵P. C. Gibbons, S. E. Schnatterly, J. J. Ritsko, and J. R. Fields, *Phys. Rev. B* **13**, 2451 (1976).
- ²⁶K. S. Singwi, M. P. Tosi, R. H. Land, and A. Sjölander, *Phys. Rev.* **176**, 589 (1968).
- ²⁷J. Hubbard, *Proc. R. Soc. London, Ser. A* **240**, 539 (1957).
- ²⁸K. N. Pathak and P. Vashishta, *Phys. Rev. B* **7**, 3649 (1973).
- ²⁹F. Brosens, L. F. Lemmens, and J. T. Devreese, *Phys. Status Solidi B* **74**, 45 (1976).
- ³⁰F. Brosens, J. T. Devreese, and L. F. Lemmens, *Phys. Status Solidi B* **80**, 99 (1977).
- ³¹J. T. Devreese, F. Brosens, and L. F. Lemmens, *Phys. Status Solidi B* **91**, 349 (1979).
- ³²B. Dabrowski, *Phys. Rev. B* **34**, 4989 (1986).
- ³³A. Holas and S. Rahman, *Phys. Rev. B* **35**, 2720 (1987).
- ³⁴E. L. Pollock and J. P. Hansen, *Phys. Rev. A* **8**, 3110 (1973).
- ³⁵M. C. Abramo and M. P. Tosi, *Nuovo Cimento Soc. Ital. Fis., B* **21**, 363 (1974).
- ³⁶A. vom Felde, J. Fink, T. Büche, B. Scheerer, and N. Nücker, *Europhys. Lett.* **4**, 1037 (1987).
- ³⁷A. vom Felde, J. Sprösser-Prou, and J. Fink, *Phys. Rev. B* **40**, 10181 (1989).
- ³⁸F. Aryasetiawan and K. Karlsson, *Phys. Rev. Lett.* **73**, 1679 (1994).
- ³⁹A. H. Reshak and S. Auluck, *Physica B* **358**, 158 (2005).
- ⁴⁰M.-T. Suzuki and H. Harima, *Physica B* **359-361**, 1180 (2005).
- ⁴¹A. R. Beal, H. P. Hughes, and W. Y. Liang, *J. Phys. C* **8**, 4236 (1975).
- ⁴²C. M. Fang, A. R. H. F. Ettema, C. Haas, G. A. Wiegers, H. van Leuken, and R. A. de Groot, *Phys. Rev. B* **52**, 2336 (1995).
- ⁴³R. Oviedo-Roa, J.-M. Martínez-Magádan, and F. Illas, *J. Phys. Chem. B* **110**, 7951 (2006).
- ⁴⁴R. Manzke, G. Crecelius, J. Fink, and R. Schöllhorn, *Solid State Commun.* **40**, 103 (1981).
- ⁴⁵U. Mackens, D. Heitmann, L. Prager, J. P. Kotthaus, and W. Beinvogl, *Phys. Rev. Lett.* **53**, 1485 (1984).
- ⁴⁶F. Stern, *Phys. Rev. Lett.* **18**, 546 (1967).
- ⁴⁷A. Yurtsever, V. Moldoveanu, and B. Tanatar, *Phys. Rev. B* **67**, 115308 (2003).
- ⁴⁸B. Ruzicka, L. Degiorgi, H. Berger, R. Gaál, and L. Forró, *Phys. Rev. Lett.* **86**, 4136 (2001).
- ⁴⁹T. Watanabe, T. Fujii, and A. Matsuda, *Phys. Rev. Lett.* **79**, 2113 (1997).
- ⁵⁰N. Nücker, U. Eckern, J. Fink, and P. Müller, *Phys. Rev. B* **44**, 7155 (1991).
- ⁵¹G. Grüner, *Density Waves in Solids* (Addison-Wesley, Reading, MA, 1994).
- ⁵²F. Denoyer, F. Comès, A. F. Garito, and A. J. Heeger, *Phys. Rev. Lett.* **35**, 445 (1975).
- ⁵³J. J. Ritsko, D. J. Sandman, A. J. Epstein, P. C. Gibbons, S. E. Schnatterly, and J. Fields, *Phys. Rev. Lett.* **34**, 1330 (1975).
- ⁵⁴L. M. Kahn, J. Ruvalds, and R. Hastings, *Phys. Rev. B* **17**, 4600 (1978).
- ⁵⁵G. Travaglini, P. Wachter, J. Marcus, and C. Schlenker, *Solid State Commun.* **37**, 599 (1981).
- ⁵⁶M. Sing, V. G. Grigoryan, G. Paasch, M. Knupfer, J. Fink, B. Lommel, and W. Aßmus, *Phys. Rev. B* **59**, 5414 (1999).